Cross-comparative analysis of evacuation behavior after earthquakes using mobile phone data

Takahiro Yabe[1¤]*, Yoshihide Sekimoto[1,2], Kota Tsubouchi[3], Satoshi Ikemoto[4]

1 Department of Civil Engineering, University of Tokyo, Tokyo, Japan, **2** Institute of Industrial Science, University of Tokyo, Tokyo, Japan, **3** Yahoo Japan Corporation, Tokyo, Japan, **4** Zenrin DataCom Corporation, Tokyo, Japan

¤ Current address: Lyles School of Civil Engineering, Purdue University, United States of America
* tyabe@purdue.edu

Abstract

Despite the importance of predicting evacuation mobility dynamics after large scale disasters for effective first response and disaster relief, our general understanding of evacuation behavior remains limited because of the lack of empirical evidence on the evacuation movement of individuals across multiple disaster instances. Here we investigate the GPS trajectories of a total of more than 1 million anonymized mobile phone users whose positions were tracked for a period of 2 months before and after four of the major earthquakes that occurred in Japan. Through a cross comparative analysis between the four disaster instances, we find that in contrast to the assumed complexity of evacuation decision making mechanisms in crisis situations, an individual's evacuation probability is strongly dependent on the seismic intensity that they experience. In fact, we show that the evacuation probabilities in all earthquakes collapse into a similar pattern, with a critical threshold at around seismic intensity 5.5. This indicates that despite the diversity in the earthquakes profiles and urban characteristics, evacuation behavior is similarly dependent on seismic intensity. Moreover, we found that probability density functions of the distances that individuals evacuate are not dependent on seismic intensities that individuals experience. These insights from empirical analysis on evacuation from multiple earthquake instances using large scale mobility data contributes to a deeper understanding of how people react to earthquakes, and can potentially assist decision makers to simulate and predict the number of evacuees in urban areas with little computational time and cost. This can be achieved by utilizing only the information on population density distribution and seismic intensity distribution, which can be observed instantaneously after the shock.

Introduction

Severe earthquakes such as the Kobe earthquake (1995), the Tohoku earthquake (2011) and more recently the Kumamoto earthquake (2016) caused mass evacuation activities owing to

considerable damage to buildings and urban infrastructure [1–4]. Human mobility prediction in disaster scenarios is crucial for various recovery efforts, including the planning of locations and capacities of evacuation shelters, and the allocation of various emergency supplies. Many of the conventional methods use urban infrastructure failure data to predict the number of evacuees in upcoming disasters. For example, the Tokyo Metropolitan Government uses a model that utilizes variables such as building collapse rate, lifeline damage rate, and inundation area data to estimate the number of evacuees [5]. However, it is difficult to use this model shortly after an earthquake because typically, several days are required for government organizations to inspect and gather information about the status of lifelines and infrastructure. In fact, after the Kumamoto earthquake (2016, magnitude 7.3), authorities failed to obtain an accurate estimate of the number of evacuees due to difficulties in data collection. This caused delays in rescue and inefficient distribution of emergency supplies [6].

Traditionally, transportation surveys were used to understand the city-scale human mobility [7]. In recent years, large scale datasets collected from mobile phones and smartphones are beginning to be utilized to understand the behavior of individuals at a low cost [8–13]. These data are used in applications in various fields such as traffic management [14–16], monitoring pandemic spreading [17], tourist mobility analysis [18] and the prediction of population distributions and dynamics [19–22]. Many works have applied this new data source for applications in disaster management [23]. Studies have shown the effect of weather patterns on human mobility [24], and its predictability using socio-economic factors [25]. In terms of understanding human mobility during larger scale disasters, a recent study analyzed call detail records to investigate the predictability of evacuation destinations of individuals after the Haiti earthquake and showed that most evacuation destinations were places that individuals have visited earlier (e.g., the home of a relative or a friend) [26]. Also, population decline was observed in various areas affected by the Tohoku Earthquake using mobile phone data [27]. Other works have used Twitter data to observe the perturbation in the radius of gyration of affected individuals during disasters [28], and to understand the tweeting behaviors of affected individuals and the transition of sentiments after large scale disasters [29, 30]. More recent studies conducted after the Nepal earthquake and Kumamoto earthquake showed that evacuation behavior could be monitored after an earthquake by using mobile phone location data (e.g. GPS, call detail records) obtained from the evacuees [31–33]. Although these works provide valuable insights into the human mobility patterns during a individual disaster case studies, they fail to provide general insights that could be applicable across different disasters. Moreover, results obtained from mobile phone data are usually delivered to decision makers several days or even weeks after the initial shocks because the use of real-time mobile phone location data is highly sensitive against privacy issues [34]. This motivates us to perform a cross-comparative analysis of human evacuation behavior after various disaster cases, to obtain a general understanding of evacuation behavior after earthquakes which can be used in planning evacuation strategies for future disasters.

Several works have performed a cross-comparative analysis across different disasters. However, to the best of our knowledge, none of the works provide analyses of detailed evacuation behavior which can be utilized by emergency management practitioners. The analysis of calling behavior after various types of disasters has shown that increase in communication after emergencies are both spatially and temporally localized, but information about emergencies spreads globally [35]. Here in this study, we focus more on the physical movements of individuals rather than communication patterns. Similar to [28], the radius of gyration of individuals across different disaster cases using Twitter Geo-tag data has been studied [36]. Although using the radius of gyration measures the perturbation of human mobility due to disasters, it does not provide direct measures of evacuation movements. In this study, we provide detailed

analysis of evacuation rates and evacuation distances of individuals after multiple earthquakes using large scale mobile phone location datasets from Japan. More specifically, we analyze the mobility of individuals who were affected by the Tohoku earthquake (2011 March) [37], Kumamoto earthquake (2016 April) [38], Nagano earthquake (2014 November) [39], and Tottori earthquake (2016 October) [40].

Data

Mobile phone location data

Yahoo Japan Corporation (https://about.yahoo.co.jp/info/en/) provides a variety of disaster notifications to users through its disaster alert app. The disaster alert app continues to acquire real-time location information of individuals in order to transmit only geographically relevant disaster notifications for individuals. The users have accepted to provide their location data when installing the application. The data is anonymized so that individuals cannot be specified, and personal information such as gender, age and occupation are unknown. Each location data is stored as a GPS record in Yahoo Japan's internal server. Each record consists of a user's unique ID (random character string), latitude, longitude, date and time. The acquisition frequency of the GPS data changes according to the movement speed of the user. If it is determined that the user is staying in a certain place for a long time, data is acquired at a relatively low frequency, and if it is determined that the user is moving, the data is acquired more frequently. By reducing the number of times data is acquired using this algorithm, it is possible to reduce the burden on the user's smartphone battery. On average, about 40 points are observed per day per user, therefore we can observe the main staying places of each individual. Currently the number of users who have installed the disaster alert app in Japan nationwide are about 1 million (Kumamoto, at 2016 April), and it is currently increasing due to the rise in disaster risk awareness. Approximately, this is 1% sample rate of the whole population which is equivalent to the national census, which is performed once in 10 years for the purpose of understanding traffic behavior. S1 Fig shows the actual GPS information for one day plotted on a white map around Kumamoto City. Each fine red dot corresponds to one GPS data. By comparing the plot with an actual map of the area, we can observe that the city center and roads that connect the surrounding cities can be traced from the data, showing its high spatial density. Table 1 shows the statistics of the disaster and also the data that were used for the experiments. We used 712,904 users' data for which an average of 19 points were observed per day for the Kumamoto earthquake. For Nagano and Tottori earthquakes, the number of users were 10244 and 24103, respectively with similar observation frequencies. We also use the GPS data set (called Konzatsu-Tokei data), provided by Zenrin Data Com (https://www.zenrin-datacom.net/en/index.html) (ZDC) to anlyze the evacuation mobility during the Tohoku earthquake. "Konzatsu-Tokei (R)" Data refers to location data collected from mobile phones using the AUTO-GPS function under the users' consent, through the "docomo map navi" service provided by NTT DOCOMO, INC. The data is processed collectively and statistically in

Table 1. Statistics of the four earthquakes and mobile phone data used for analysis.

Disaster	Disaster Statistics			Data Statistics	
	Date	Max. SI	No. LGUs (SI$\geq$4.0)	Obs. Period	No. Users
Tohoku Earthquake	2011/3/11	6.6	140	2011/02/01 $\sim$ 03/31	157,225
Kumamoto Earthquake	2016/4/16	6.7	153	2016/03/15 $\sim$ 05/15	712,901
Tottori Earthquake	2016/10/21	5.7	19	2016/10/01 $\sim$ 11/30	24,103
Nagano Earthquake	2014/11/22	5.7	10	2014/11/01 $\sim$ 12/30	10,244

https://doi.org/10.1371/journal.pone.0211375.t001
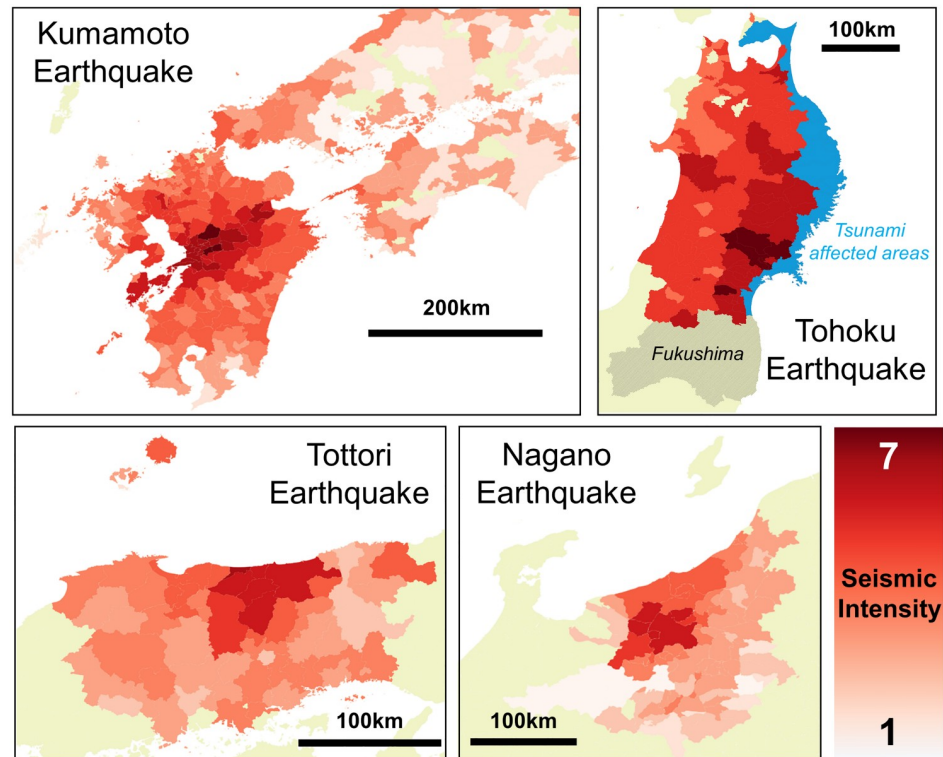
Fig 1. Areas that were analyzed in the four earthquakes (red). Seismic intensity values observed in each municipality is shown by the darkness of red colors. Note that for the Tohoku Earthquake, the coastal areas in Aomori, Iwate and Miyagi prefectures (blue) and areas in Fukushima prefecture that were affected by the nuclear power plant accident was removed from the analysis.

order to ananymize and to conceal private information. GPS data (latitude, longitude) of smartphones are collected approximately every 5 minutes at most and does not include other personal information such as gender and age. To analyze the evacuation behaviors of people at the time of the Tohoku earthquake, we used the data from February 1, 2011 to March 31, 2011, and the total number of IDs in the Tohoku region (Aomori, Iwate, Akita, Miyagi, and Yamagata prefectures) was 157,225. To analyze the evacuation behavior due to the effects of earthquakes and to separate the effects of other disaster types, we excluded areas that were hit by the tsunami (coastal areas) shown in blue color in Fig 1 and cities in Fukushima, which were heavily affected by the nuclear power plant accident.

Seismic intensity data

"Seismic intensity" is used as an index to measure the strength of the external force of earthquakes, varying from 1 (very small) to 7 (extreme shock), with 0.1 increments. Mashiki City experienced the largest seismic intensity of 6.7 during the Kumamoto earthquake. Seismic intensity is obtained from the acceleration caused by the earthquake, and each local government unit is given a seismic intensity value. The seismic intensity data is published in the "Jishin/Kazan Geppou (Monthly magazine of earthquakes and volcanoes)" published by the Japan Meteorological Agency (https://www.data.jma.go.jp/svd/eqev/data/gaikyo/ (in Japanese)). Note that seismic intensity is different from "magnitude", which is only observed at the epicenter. We used the data from 2016 April and October, 2014 November, and 2011 March. Fig 1 shows the seismic intensity data for each local government unit (LGU).

Data analysis and results

Home location estimation and evacuation

It is well known that human trajectories show a high degree of temporal and spatial regularity, each individual having a significant probability to return to a few highly frequented locations, including his/her home location [11]. Due to this characteristic, it has been shown that home locations of individuals can be detected with high accuracy by clustering the individual's stay point locations over night [12]. The home location of each individual was detected by applying mean-shift clustering to the nighttime staypoints (observed between 8PM and 6AM), weighted by the duration of stays in each location [41, 42]. Mean shift clustering was implemented using the scikit-learn package on Python (http://scikit-learn.org/stable/modules/generated/sklearn. cluster.MeanShift.html). An individual was detected to be evacuated if the individual is estimated to be staying more than r (meters) away from his or her estimated home location. Evacuation rate on a given day in a given city is calculated by dividing the number of evacuated individuals by the total number of users that were estimated to be living in that city. For each disaster d, we calculate the evacuation rate $p_d(z)$ at a given seismic intensity z by the following equation.

$$p_d(z) = \frac{\sum_{i \in S_d(z)} M_i^*}{\sum_{i \in S_d(z)} M_i} \tag{1}$$

where $S_d(z)$ is the set of LGUs that experienced a seismic intensity of z in disaster d, M_i is the total number of users living in LGU i, and M_i^* is the number of evacuated people from LGU i, which we observe from trajectories of mobile phone location data.

Accuracy of mobile phone location data

The mobile phone data has a sample rate of about 1%, which is about the same as the sample rate of the personal trip survey conducted by the Ministry of Land, Infrastructure and Transport, so it is suggested that this sample rate is enough for grasping the entire urban flow. Moreover, studies have shown that the distribution of the entire population can be accurately reproduced from the call detail record data obtained from mobile phones [19]. To show that our data is also sufficient to represent the whole population, we examine how accurate the actual population distribution can be estimated from the nighttime GPS data. As verification data, we use the national census data, which contains the residential population data for every 1,000 meter grid. We separate Kumamoto Prefecture into 1,000 meter grid, and we estimate the population in each grid mesh by multiplying the number of IDs in the grid mesh from the GPS dataset by the inverse of the sample rate. The correlation coefficient between the estimated population and the actual population is 0.853, showing a high accuracy of population estimation (S2 Fig).

Spatial analysis of seismic intensity and evacuation

Fig 2 shows the spatial distribution of seismic intensity (A) and evacuation rate (B) after the Kumamoto earthquake. Both data are aggregated into local government unit (LGU) areas. The evacuation rate in a given LGU is calculated by dividing the estimated number of individuals who are staying more than 200 meters away from their estimated home location after the earthquake by the total number of individuals who are estimated to be living in the given LGU. We can observe that even though seismic intensity gradually attenuates as the distance from the epicenter increases, evacuation rate abruptly decreases from approximately 40% to less than 10% around areas with a seismic intensity of 5.0. We can infer that human evacuation

A **Seismic Intensity**   **B** **Evacuation Rate (%)**
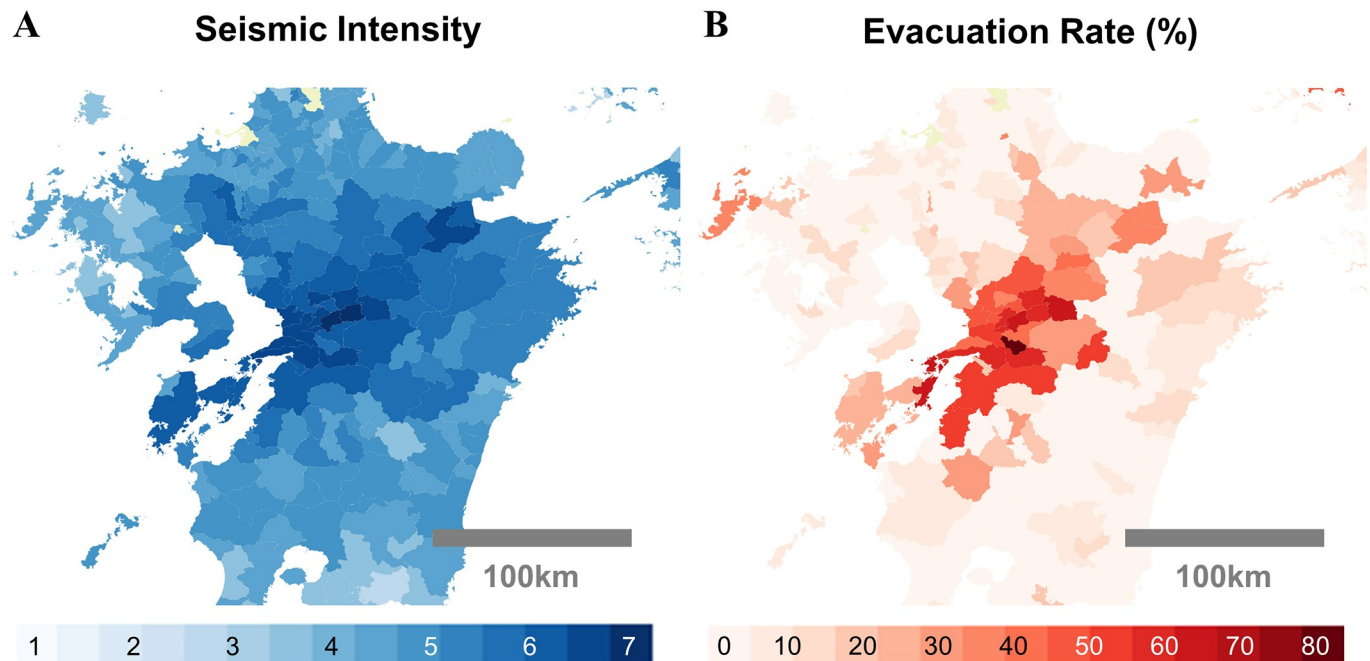
Fig 2. Spatial distribution of the seismic intensity and evacuation rates during the Kumamoto earthquake. A: seismic intensity data shown for each local government unit (LGU). B: evacuation rate for each LGU. The seismic intensity and evacuation rates are positively correlated, however, the evacuation rates suddenly increase at around 5.

https://doi.org/10.1371/journal.pone.0211375.g002

activity has a critical 'tipping point' with respect to seismic intensity. The underlying reasons for this behavior are not trivial. However, it can be assumed that evacuation activities increase sharply owing to the collapse of buildings and critical social infrastructure such as electricity and gas lines, which occur at similar seismic intensities. We model this nonlinear characteristic of evacuation activities by further observing the evacuation activities for four large earthquakes in Japan.

Fragility curve for evacuation behavior

To explore the general properties of the evacuation activities after large earthquakes, we analyzed each individual's movement after the initial shocks of the four earthquakes. Out of these earthquakes, the Tohoku earthquake caused multiple types of hazards including a tsunami and a nuclear power plant accident. In this study, we focus on areas that were affected only by the earthquake to understand the evacuation behavior caused by large earthquakes. Therefore, the LGUs in the Fukushima prefecture and the LGUs along the coastal line in the Tohoku region are beyond the scope of this study [43]. For other earthquakes, we calculated the evacuation rate of all LGUs that experienced a seismic intensity of larger than 4.0. Fig 3A shows the evacuation rates during the four earthquakes according to their seismic intensities. The four different colors and plots correspond to the different earthquakes. To model the sudden increase of evacuation rates with respect to seismic intensities, we use the fragility curve model.

The fragility curve is a model used in the field of structural mechanics, mainly for modelling the collapse rate of a building with respect to seismic intensities of earthquakes and the inundation height of tsunami [44]. The external force of the disaster is taken on the horizontal axis and the vertical axis is the collapse rate. It was found that the inundation depth of the tsunami and the collapse rate of the building follow a cumulative log normal distribution function [44].
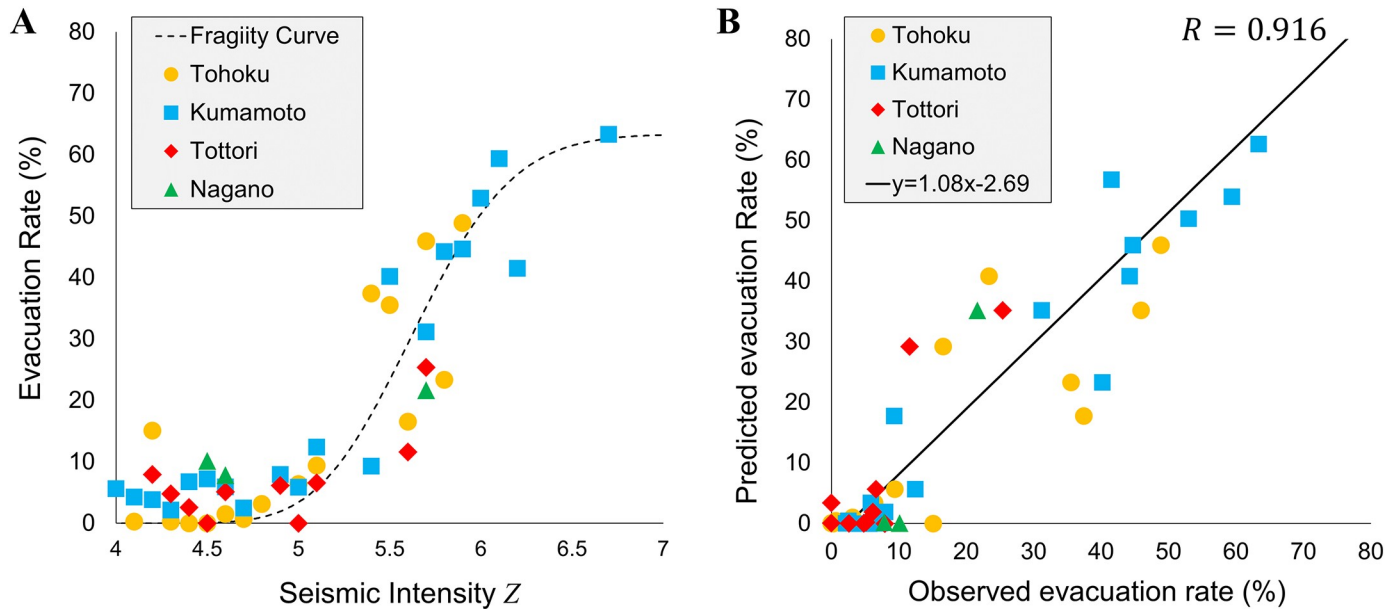
Fig 3. Fragility curves for evacuation rates. A: evacuation rates for each of the four earthquakes plotted against seismic intensities for all affected LGUs, along with the estimated fragility curve. Colors indicate earthquake incident. B: scatter plot of estimated and true evacuation rates.

Similarly, it was also found that the seismic intensity of the earthquake and the collapse rate of the building can also be approximated with a cumulative log normal distribution function [45]. The common feature of both discoveries is that the collapse rate of buildings is close to 0 up to a certain external force but rapidly increases from a certain inflection point. The cumulative log normal distribution is a function that can model this sudden increase. The cumulative log normal distribution function is a function shown in equation, and there are three parameters (μ, σ, a). μ and σ dictate the slope of the function and the position of the inflection point, while a determines the maximum value of evacuation rates. We model the evacuation rate of humans $p(z)$ given seismic intensity z as the following fragility function, and estimate parameters $\hat{\mu}, \hat{\sigma}, \hat{a}$ using the maximum likelihood estimation approach [45] given the observations from mobile phone data.

$$p(z) = a\Phi\left(\frac{\ln z - \mu}{\sigma}\right) = a\int_0^z \frac{1}{z\sqrt{2\pi}\sigma}\exp\left(\frac{-(\ln z - \mu)^2}{2\sigma^2}\right)dz \qquad (2)$$

The estimated parameters of the fragility curve using the four disaster cases are $\mu = 1.73$, $\sigma = 0.075$, $a = 0.63$, and the correlation coefficient between the model and the data was $R = 0.916$, as shown in Fig 3B. From these estimations, we can infer that the seismic intensity at which individuals start to evacuate is approximately 5.2 and evacuation rate increases sharply between intensities of 5.5 and 6.0. At a seismic intensity of approximately 6.5, evacuation rate plateaus at 63%. This plateau explains the strength of the infrastructure in Japan because it implies that regardless of seismic intensity, a relatively large fraction (approximately 34%) of the individuals do not have to evacuate from their homes. We test the robustness of our results by performing a leave-one-out test similar to cross validation. More specifically, we estimate the parameters of the fragility curve using data obtained from three earthquakes, and then test the fit for the left out earthquake by measuring the correlation coefficient R and mean average percentage error (MAPE) of evacuation rates. Table 2 shows the robustness testing results. The

Table 2. Robustness test of fragility curve fitting results. The evacuation rates for the "left out earthquake" was predicted by the model fitted by the other three earthquakes.

Earthquake left out for prediction	Prediction Performance		Estimated parameters	
	R	MAPE (%)	$\hat{\mu}$	$\hat{\sigma}$
Tohoku	0.879	5.35	1.79	0.122
Kumamoto	0.944	7.04	1.86	0.185
Tottori	0.822	4.92	1.81	0.144
Nagano	0.984	7.91	1.80	0.137

first row means that the parameters of the fragility curve were estimated using data from disasters except Tohoku earthquake (i.e. Kumamoto, Tottori, Nagano earthquakes) as $\hat{\mu} = 1.79$ and $\hat{\sigma} = 0.122$, and were used to predict the evacuation rates after the Tohoku earthquake, which showed high accuracy ($R = 0.879$, MAPE = 5.35%). For all disasters, prediction showed high correlation and small MAPE, all below 10%. Moreover, the estimated parameters were similar for all testing cases, showing the high stability and robustness of the estimated fragility curve. This test shows that by using the fragility curve fitted by data from past disasters, we are able to predict the evacuation rates in future disasters with high precision.

Understanding the spatial and temporal characteristics of evacuation behavior is important for creating effective evacuation plans. We investigated the evacuation distance, which is shown in Fig 4. The long tail distribution of the evacuation distance follows a power law $P(d) = \alpha d^{-\gamma}$, similar to cases in non-disaster cases [11]. We can observe the evacuation distance to be
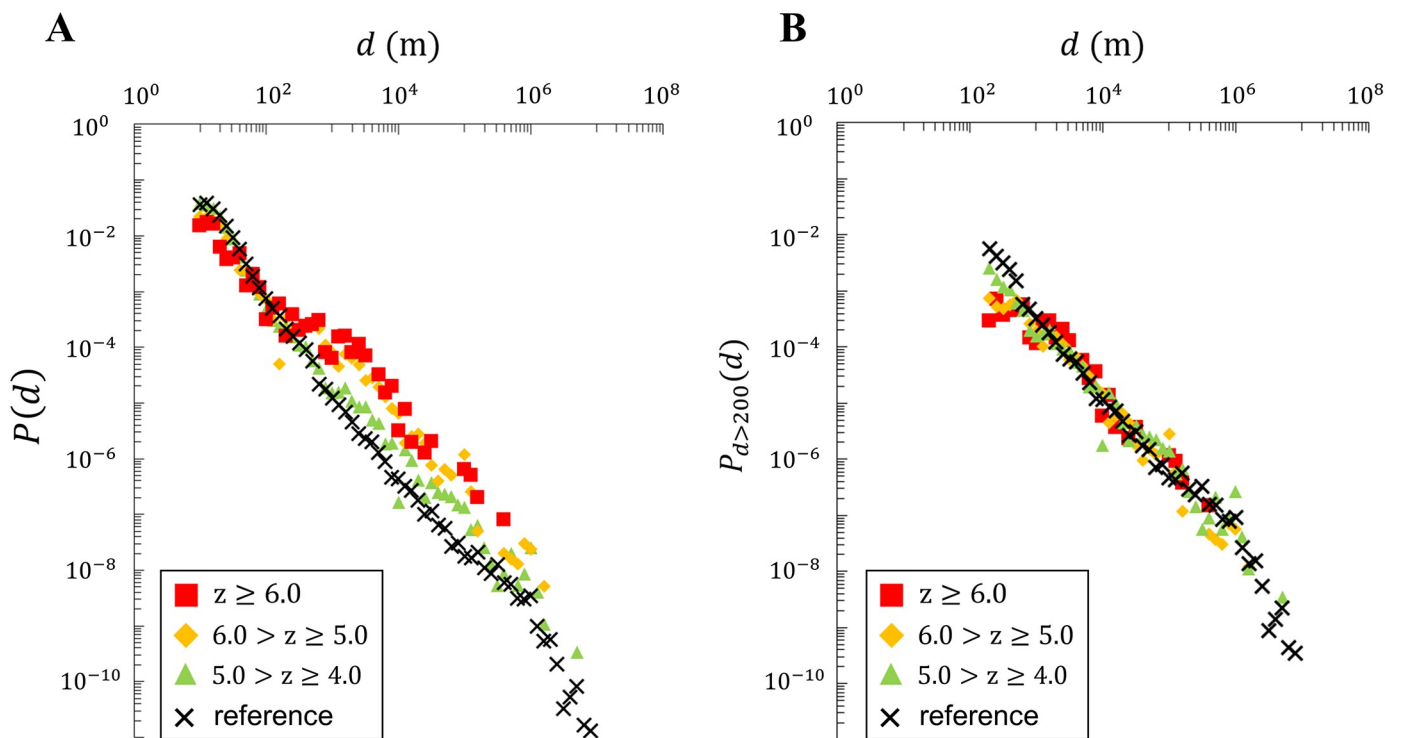
Fig 4. Distribution of evacuation distance. A: distribution of evacuation distances including all observed users. B: distribution of evacuation distances for only those who evacuated. We can observe that the probability densities for different seismic intensities collapse into one distribution, implying that evacuation distances are not dependent on seismic intensity.

between 1 kilometer to 1000 kilometers for all levels of seismic intensities. Moreover, when we cutoff the individuals who did not evacuate and plot the evacuation distance distributions for only the evacuated individuals (i.e. $d > 200$), we can observe that the distance distribution collapse into one distribution despite different seismic intensities with $1.13 \leq \gamma \leq 1.38$. This implies that if individuals decide to evacuate from their homes, their destination is not affected by the intensity of the earthquake. Moreover, this shows that individuals have limited options for destinations, such as evacuation shelters and the houses of their relatives, which reinforces the findings from the study of Haiti Earthquake [26]. Through our cross-comparative analysis, we were able to expand this finding to a general setting.

Conclusion

Using large scale mobility data collected from over 1 million mobile phones of users affected by earthquakes, we carried out a cross-comparative analysis on the evacuation mobility patterns of individuals. Through a cross comparison across four large scale earthquakes in Japan, we found that although city characteristics vary, the evacuation rates can be approximated well with a single fragility curve with respect to seismic intensities, with a high correlation of $R = 0.916$. The robustness of the fragility curve was checked by performing a cross-validation test on the four disasters. Moreover, it was found that the distribution of evacuation distances did not depend on the seismic intensity that the individual experienced, which extends the past findings to a general setting. Our data-driven analysis of evacuation behavior after earthquakes based on seismic intensity could improve the manner in which disaster managers prepare and respond to disasters. Since seismic intensity data can be obtained instantly after the shock, practitioners can use that information to predict the approximate number of evacuees instantaneously after the earthquake to develop evacuation shelter location plans and significantly improve the quality of disaster response. Our future works include analyzing the fragility curves of evacuation rates in different areas of the world apart from Japan to investigate the factors that characterize robustness of cities against earthquakes.

Supporting information

S1 Fig. Mobile phone location data. Left: GPS data obtained during 1 day plotted onto a white map in Kumamoto area. Right: OpenStreetMap data of Kumamoto area, showing the road networks [46]. The mobile phone data is dense in both spatial and temporal aspects to analyze the detailed mobility of individuals.
(PNG)

S2 Fig. Comparison between national census data and population density estimated from GPS data. Estimated population and the population obtained from the census. The blue dots correspond to one grid mesh (1000m size) respectively.
(PNG)

S3 Fig. Sensitivity analysis on *r*. Fragility curves with different *r* parameter values. Although the estimated parameters vary under different parameters, the general findings are not affected, where the fragility curves fit the result well.
(TIF)

S4 Fig. Evacuation timing after earthquake. Evacuation timing of individuals after the Kumamoto earthquake. Results show that the higher the seismic intensity, individuals evacuate more quickly.
(TIF)

Acknowledgments

Author Contributions

Conceptualization: Takahiro Yabe, Yoshihide Sekimoto, Kota Tsubouchi, Satoshi Ikemoto.

Data curation: Takahiro Yabe, Kota Tsubouchi, Satoshi Ikemoto.

Formal analysis: Takahiro Yabe, Kota Tsubouchi.

Investigation: Takahiro Yabe, Kota Tsubouchi.

Methodology: Takahiro Yabe.

Supervision: Yoshihide Sekimoto, Kota Tsubouchi.

Validation: Takahiro Yabe.

Visualization: Takahiro Yabe.

Writing – original draft: Takahiro Yabe, Yoshihide Sekimoto, Kota Tsubouchi, Satoshi Ikemoto.

Writing – review & editing: Takahiro Yabe, Yoshihide Sekimoto, Kota Tsubouchi, Satoshi Ikemoto.

References

1. Yun NY, Hamada M. Evacuation behavior and fatality rate during the 2011 Tohoku-Oki earthquake and tsunami. Earthquake Spectra. 2015; 31(3):1237–1265. https://doi.org/10.1193/082013EQS234M

2. Heath R. The Kobe earthquake: Some realities of strategic management of crises and disasters. Disaster Prevention and Management: An International Journal. 1995; 4(5):11–24. https://doi.org/10.1108/09653569510100965

3. Chiaro G, Alexander G, Brabhaharan P, Massey C, Koseki J, Yamada S, et al. Reconnissance report on geotechnical and geological aspects of the 14-16 April 2016 Kumamoto earthquakes, Japan. 2017.

4. Mimura N, Yasuhara K, Kawagoe S, Yokoki H, Kazama S. Damage from the Great East Japan Earthquake and Tsunami-a quick report. Mitigation and adaptation strategies for global change. 2011; 16(7):803–818. https://doi.org/10.1007/s11027-011-9297-7

5. Tokyo Metropolitan Government. Report on Damage Estimates in Tokyo Due to an Earthquake Directly Hitting Tokyo; 2012; Accessed 13 October 2018. http://www.bousai.metro.tokyo.jp/foreign/english/taisaku/2002029/2002030.html.

6. Mainichi Newspaper. Evacuation center at Grand Messe Kumamoto; 2016; Accessed 13 October 2018. https://mainichi.jp/articles/20160418/k00/00m/040/102000c.

7. Sekimoto Y, Shibasaki R, Kanasugi H, Usui T, Shimazaki Y. Pflow: Reconstructing people flow recycling large-scale social survey data. IEEE Pervasive Computing. 2011; 10(4):27–35. https://doi.org/10.1109/MPRV.2011.43

8. Phithakkitnukoon S, Smoreda Z, Olivier P. Socio-geography of human mobility: A study using longitudinal mobile phone data. PloS one. 2012; 7(6):e39253. https://doi.org/10.1371/journal.pone.0039253 PMID: 22761748

9. Jiang S, Yang Y, Gupta S, Veneziano D, Athavale S, González MC. The TimeGeo modeling framework for urban mobility without travel surveys. Proceedings of the National Academy of Sciences. 2016; 113(37):E5370–E5378. https://doi.org/10.1073/pnas.1524261113

10. Wardrop N, Jochem W, Bird T, Chamberlain H, Clarke D, Kerr D, et al. Spatially disaggregated population estimates in the absence of national population and housing census data. Proceedings of the National Academy of Sciences. 2018; 115(14):3529–3537. https://doi.org/10.1073/pnas.1715305115

11. Gonzalez MC, Hidalgo CA, Barabasi AL. Understanding individual human mobility patterns. nature. 2008; 453(7196):779. https://doi.org/10.1038/nature06958 PMID: 18528393

12. Calabrese F, Di Lorenzo G, Liu L, Ratti C. Estimating Origin-Destination flows using opportunistically collected mobile phone location data from one million users in Boston Metropolitan Area. IEEE Pervasive Computing. 2011; 10(4):36–44.

13. Phithakkitnukoon S, Horanont T, Di Lorenzo G, Shibasaki R, Ratti C. Activity-aware map: Identifying human daily activity pattern using mobile phone data. In: International Workshop on Human Behavior Understanding. Springer; 2010. p. 14–25.

14. Iqbal MS, Choudhury CF, Wang P, González MC. Development of origin–destination matrices using mobile phone call data. Transportation Research Part C: Emerging Technologies. 2014; 40:63–74. https://doi.org/10.1016/j.trc.2014.01.002

15. Wang P, Hunter T, Bayen AM, Schechtner K, González MC. Understanding road usage patterns in urban areas. Scientific reports. 2012; 2:1001. https://doi.org/10.1038/srep01001 PMID: 23259045

16. Demissie MG, de Almeida Correia GH, Bento C. Intelligent road traffic status detection system through cellular networks handover information: An exploratory study. Transportation research part C: emerging technologies. 2013; 32:76–88. https://doi.org/10.1016/j.trc.2013.03.010

17. Bengtsson L, Lu X, Thorson A, Garfield R, Von Schreeb J. Improved response to disasters and outbreaks by tracking population movements with mobile phone network data: a post-earthquake geospatial study in Haiti. PLoS medicine. 2011; 8(8):e1001083. https://doi.org/10.1371/journal.pmed.1001083 PMID: 21918643

18. Phithakkitnukoon S, Horanont T, Witayangkurn A, Siri R, Sekimoto Y, Shibasaki R. Understanding tourist behavior using large-scale mobile sensing approach: A case study of mobile phone users in Japan. Pervasive and Mobile Computing. 2015; 18:18–39. https://doi.org/10.1016/j.pmcj.2014.07.003

19. Deville P, Linard C, Martin S, Gilbert M, Stevens FR, Gaughan AE, et al. Dynamic population mapping using mobile phone data. Proceedings of the National Academy of Sciences. 2014; 111(45):15888–15893. https://doi.org/10.1073/pnas.1408439111

20. Shimosaka M, Maeda K, Tsukiji T, Tsubouchi K. Forecasting urban dynamics with mobility logs by bilinear Poisson regression. In: Proceedings of the 2015 ACM international joint conference on pervasive and ubiquitous computing. ACM; 2015. p. 535–546.

21. Nishi K, Tsubouchi K, Shimosaka M. Hourly pedestrian population trends estimation using location data from smartphones dealing with temporal and spatial sparsity. In: Proceedings of the 22nd ACM SIGSPATIAL International Conference on Advances in Geographic Information Systems. ACM; 2014. p. 281–290.

22. Noulas A, Scellato S, Lambiotte R, Pontil M, Mascolo C. A tale of many cities: universal patterns in human urban mobility. PloS one. 2012; 7(5):e37027. https://doi.org/10.1371/journal.pone.0037027 PMID: 22666339

23. Gething PW, Tatem AJ. Can mobile phone data improve emergency response to natural disasters? PLoS medicine. 2011; 8(8):e1001085. https://doi.org/10.1371/journal.pmed.1001085 PMID: 21918644

24. Horanont T, Phithakkitnukoon S, Leong TW, Sekimoto Y, Shibasaki R. Weather effects on the patterns of people's everyday activities: a study using GPS traces of mobile phone users. PloS one. 2013; 8(12): e81153. https://doi.org/10.1371/journal.pone.0081153 PMID: 24367481

25. Yabe T, Tsubouchi K, Sudo A, Sekimoto Y. Predicting irregular individual movement following frequent mid-level disasters using location data from smartphones. In: Proceedings of the 24th ACM SIGSPATIAL International Conference on Advances in Geographic Information Systems. ACM; 2016. p. 54.

26. Lu X, Bengtsson L, Holme P. Predictability of population displacement after the 2010 Haiti earthquake. Proceedings of the National Academy of Sciences. 2012; 109(29):11576–11581. https://doi.org/10.1073/pnas.1203882109

27. Song X, Zhang Q, Sekimoto Y, Horanont T, Ueyama S, Shibasaki R. Intelligent system for human behavior analysis and reasoning following large-scale disasters. IEEE Intelligent Systems. 2013; 28(4):35–42. https://doi.org/10.1109/MIS.2013.35

28. Wang Q, Taylor JE. Quantifying human mobility perturbation and resilience in Hurricane Sandy. PLoS one. 2014; 9(11):e112608. https://doi.org/10.1371/journal.pone.0112608 PMID: 25409009

29. Kryvasheyeu Y, Chen H, Moro E, Van Hentenryck P, Cebrian M. Performance of social network sensors during Hurricane Sandy. PLoS one. 2015; 10(2):e0117288. https://doi.org/10.1371/journal.pone.0117288 PMID: 25692690

30. Kryvasheyeu Y, Chen H, Obradovich N, Moro E, Van Hentenryck P, Fowler J, et al. Rapid assessment of disaster damage using social media activity. Science advances. 2016; 2(3):e1500779. https://doi.org/10.1126/sciadv.1500779 PMID: 27034978

31. Horanont T, Witayangkurn A, Sekimoto Y, Shibasaki R. Large-scale auto-GPS analysis for discerning behavior change during crisis. IEEE Intelligent Systems. 2013; 28(4):26–34. https://doi.org/10.1109/MIS.2013.3

32. Yabe T, Tsubouchi K, Sudo A, Sekimoto Y. Estimating Evacuation Hotspots using GPS data: What happened after the large earthquakes in Kumamoto, Japan. In: Proc. of the 5th International Workshop on Urban Computing; 2016.

33. Wilson R, zu Erbach-Schoenberg E, Albert M, Power D, Tudge S, Gonzalez M, et al. Rapid and near real-time assessments of population displacement using mobile phone data following disasters: the 2015 Nepal Earthquake. PLoS currents. 2016; 8. https://doi.org/10.1371/currents.dis.d073fbece328e4c39087bc086d694b5c PMID: 26981327

34. De Montjoye YA, Hidalgo CA, Verleysen M, Blondel VD. Unique in the crowd: The privacy bounds of human mobility. Scientific reports. 2013; 3:1376. https://doi.org/10.1038/srep01376 PMID: 23524645

35. Bagrow JP, Wang D, Barabasi AL. Collective response of human populations to large-scale emergencies. PloS one. 2011; 6(3):e17680. https://doi.org/10.1371/journal.pone.0017680 PMID: 21479206

36. Wang Q, Taylor JE. Patterns and limitations of urban human mobility resilience under the influence of multiple types of natural disaster. PLoS one. 2016; 11(1):e0147299. https://doi.org/10.1371/journal.pone.0147299 PMID: 26820404

37. Hirose F, Miyaoka K, Hayashimoto N, Yamazaki T, Nakamura M. Outline of the 2011 off the Pacific coast of Tohoku Earthquake (M w 9.0)—Seismicity: foreshocks, mainshock, aftershocks, and induced activity—. Earth, planets and space. 2011; 63(7):1. https://doi.org/10.5047/eps.2011.05.019

38. Shirahama Y, Yoshimi M, Awata Y, Maruyama T, Azuma T, Miyashita Y, et al. Characteristics of the surface ruptures associated with the 2016 Kumamoto earthquake sequence, central Kyushu, Japan. Earth, Planets and Space. 2016; 68(1):191. https://doi.org/10.1186/s40623-016-0559-1

39. Lin A, Sano M, Yan B, Wang M. Co-seismic surface ruptures produced by the 2014 Mw 6.2 Nagano earthquake, along the Itoigawa–Shizuoka tectonic line, central Japan. Tectonophysics. 2015; 656:142–153. https://doi.org/10.1016/j.tecto.2015.06.018

40. Kagawa T, Noguchi T, Yoshida S, Yamamoto S. Effect of the surface geology on strong ground motions due to the 2016 Central Tottori Earthquake, Japan. Earth, Planets and Space. 2017; 69(1):106. https://doi.org/10.1186/s40623-017-0689-0

41. Ashbrook D, Starner T. Using GPS to learn significant locations and predict movement across multiple users. Personal and Ubiquitous computing. 2003; 7(5):275–286. https://doi.org/10.1007/s00779-003-0240-0

42. Kanasugi H, Sekimoto Y, Kurokawa M, Watanabe T, Muramatsu S, Shibasaki R. Spatiotemporal route estimation consistent with human mobility using cellular network data. In: Pervasive Computing and Communications Workshops (PERCOM Workshops), 2013 IEEE International Conference on. IEEE; 2013. p. 267–272.

43. Tsubokura M, Kato S, Nihei M, Sakuma Y, Furutani T, Uehara K, et al. Limited internal radiation exposure associated with resettlements to a radiation-contaminated homeland after the Fukushima Daiichi nuclear disaster. Plos one. 2013; 8(12):e81909. https://doi.org/10.1371/journal.pone.0081909 PMID: 24312602

44. Koshimura S, Oie T, Yanagisawa H, Imamura F. Developing fragility functions for tsunami damage estimation using numerical model and post-tsunami data from Banda Aceh, Indonesia. Coastal Engineering Journal. 2009; 51(03):243–273. https://doi.org/10.1142/S0578563409002004

45. Baker JW. Efficient analytical fragility function fitting using dynamic structural analysis. Earthquake Spectra. 2015; 31(1):579–599. https://doi.org/10.1193/021113EQS025M

46. OpenStreetMap contributors. Planet dump retrieved from https://planet.osm.org; 2017. https://www.openstreetmap.org.